

## Detection of the polarization spatial distribution of THz radiation generated by two-color laser filamentation

S. V. Smirnov, M. S. Kulya, A. N. Tsyarkin, S. E. Putilin, V. G. Bespalov

ITMO University, Kronverkskiy, 49, St. Petersburg, 197101, Russia

smirnov.semen@niuitmo.ru, mskulya@corp.ifmo.ru, tsypkinan@mail.ru,  
seputilin@yandex.ru, victorbespaloff@gmail.com

PACS 52.38.-r, 42.25.Ja

DOI 10.17586/2220-8054-2017-8-5-613-619

The spatial distribution of the terahertz radiation polarization is experimentally measured from a femtosecond laser two-color filament in air. Terahertz radiation generation from two-color plasma filamentation with a  $\beta$ -BBO crystal located behind the lens leads to the spatial inhomogeneity of the polarization distribution. Inhomogeneity of the terahertz field polarization is determined by the polarization of the fundamental harmonic of the pump radiation after passing through the  $\beta$ -BBO crystal. A spatial inhomogeneity of the fundamental harmonic polarization is observed owing to the  $\beta$ -BBO crystal acting as a phase plate illuminated by a spherical front.

**Keywords:** filament generation, terahertz radiation, polarization.

*Received: 18 August 2017*

*Revised: 21 August 2017*

### 1. Introduction

Terahertz radiation (THz) is widely applied in biological diagnostics systems [1], chemistry [2], holography [3–5] and imaging [6, 7]. There are three main types of THz generation methods with femtosecond pulse pumping: nonlinear optical rectification [8], generation from the surface of a semiconductor layer based on the Dember effect (or by means of a photoconductive antenna) and femtosecond-laser-beam filamentation [9, 10]. One of the attractive features of filamentation is that the THz bandwidth is only determined by the exciting pulse duration and can reach up to 100 THz [11]. Filamentation deserves attention because it allows the generation of high-intensity THz radiation and management of its properties (intensity, polarization and radiation pattern) by varying the pump pulse duration and focusing conditions [12, 13]. The physical origin of the THz radiation is attributed to the transition Cherenkov emission process [14, 15]. One of the important properties of THz radiation is the polarization state. Previously [14, 16], it has been shown that the integrated field of the THz beam has a radial polarization. In the latest research, these results have been supplemented with the fact that the polarization of the THz field has an elliptic structure [17, 18]. This fact can be explained by a four-wave optical rectification [19]. The ellipticity of the integrated THz field polarization was recorded for the case of two-color filamentation [20, 21]. Moreover, it has been shown that THz radiation polarization is directly dependent on the polarization of the fundamental pump radiation [18]. However, all of this research was performed for an integrated THz beam profile and did not consider the possibility of mapping the local polarization of the THz beam. Recent research [22] demonstrated a method for generating broadband and few-cycle THz vortex beams through conversion of a radially polarized THz beam into a THz vortex beam. Thus, the polarization behavior in THz beams gains additional importance in the singular optics of THz spectral range [23, 24].

The current state of this technology demonstrates that it is possible to obtain a spatial distribution of the THz field in the time domain at different beam points independently and thus enables the mapping of the local properties of the investigated field, which is important in various imaging applications. In our research, we experimentally record the dependency of the polarization spatial distribution of the THz radiation generated in two-color filamentation. We identify the local THz field polarization inhomogeneity which is related to the inhomogeneity of the spatial distribution of laser fundamental pumping polarization state. Using this method, one can control the polarization inhomogeneity and thus vary the beam shape. One of the possible applications of such beam shaping is vortex beam generation, which can be realized by determining the polarization state distribution. Based on this method, the vortex beam properties can be used in a THz holographic imaging system [25].

## 2. Experimental setup and results

The pump radiation in the femtosecond laser system exhibited the following parameters: central wavelength of 800 nm, repetition rate of 1 kHz, pulse duration of 35 fs, pulse energy of 2 mJ, as well as horizontal polarization. To generate a filament, the femtosecond radiation was focused by a lens with a focal length of 25 cm. The  $\beta$ -BBO crystal with 300  $\mu\text{m}$  thickness placed behind the lens focus was used for the second-harmonic generation. The  $\beta$ -BBO crystal was cut for type-I phase-matched second-harmonic generation with 800 nm pump light. Owing to the fact that the crystal was in a spherical beam, the efficiency of the second harmonic conversion for the horizontal and vertical polarization of the fundamental harmonic was 1 %. However, as described previously [26], the properties of the THz beam profile radiation can be regulated by varying the distance from the BBO to the filament, the azimuthal angle of BBO, the tilt angle of BBO and the tilt angle of the focusing lens. In our case, we determined the optimal parameters for the  $\beta$ -BBO crystal position as being when a maximum THz signal was observed. The filament length was measured from a photograph on the CCD camera and the value was approximately 15 mm. The polarization of the two-color radiation output is presented in Fig. 1(a,b). The orientation of the fundamental harmonic was set by the rotation of the half-wave plate at  $90^\circ$  before the focusing lens (L). Before measuring the polarization of the fundamental pump and the second harmonic, we reduced the pump radiation power so that there was no filamentation, and made experimental measurements at the correlating points of the space with terahertz radiation. Polarization and ellipticity measurements were made using a polarizer (Glan prism) fixed in rotational motion to determine the angle of inclination of the polarization, and a power meter to measure ellipticity. In the first case, the initial horizontal polarization of the fundamental harmonic passed through the  $\beta$ -BBO crystal and then was rotated at the angle  $\alpha = -15^\circ$  in relation to the initial horizontal polarization axis of 800 nm. In the second case, the ellipticity in the beam profile was 0.12 (Fig. 2(b-I)) and the initial vertical polarization after passing through the  $\beta$ -BBO crystal was rotated at the angle  $\alpha = 73^\circ$  with an ellipticity in the beam profile of 0.22 (Fig. 2(b-II)). The polarization of the second harmonic after the  $\beta$ -BBO crystal in both cases was linear, and its orientation was  $\beta = 73^\circ$  (Fig. 2(b-I,II)).

The THz radiation was collimated by the parabolic mirror with a 10 cm focal length and 10 cm aperture size (PM 1). It was then focused by the second parabolic mirror (PM 2) on a 1 mm-thick  $\langle 110 \rangle$  oriented ZnTe crystal [27]. The 35 fs, 800 nm pulse in conjunction with 300  $\mu\text{m}$ -thick Type-I  $\beta$ -BBO should result in a THz emission with at least a 20 THz bandwidth. However, we used ZnTe with 1 mm-thickness, which has an acceptance bandwidth only up to 2 THz (Fig. 2(b-II)). The 1 mm-thick Teflon filter (F), placed between the mirrors, attenuated the white light radiation generated by the filament and the radiation of the fundamental and second harmonics. To obtain the THz amplitude as a function of time, we used a standard scheme of the electro-optical detection, consisting of a quarter-wave plane, a Wollaston prism (WP) and a balance detector (BD). The spatial dependence of the THz field polarization was measured by moving the diaphragm (D), connected to a THz polarizer (THzP) (wire grid) placed after the Teflon filter inside the collimated beam. Such an approach has been shown previously [3,28], even though it exhibits faster fall-off of the registered signal when moving from the center to the edge owing to the change of the angle between the signal wave vector and the optical axis. The projection of the signal is proportional to the cosine of this angle. The THz field intensity had a conical form [29] and the THz field measurement was performed on the maximum intensity of the ring.

Previously [19,30], the elliptical polarization of the THz radiation has been demonstrated for the two orthogonal polarization axes. The ellipticity parameter (eccentricity and main axis tilt) can be obtained by decomposing the two orthogonal polarizations. Fig. 1(c) demonstrates the measured THz field amplitude for two orthogonal polarization states, when a THz polarizer placed in a wide collimated beam is horizontally orientated (X state is  $0^\circ$ ), and vertically orientated (Y state is  $90^\circ$ ). The X-Y graph shows a closed curve, which can be depicted by the ellipse with an ellipticity parameter and an axis tilt [17,18]. Fig. 1 demonstrates the THz pulse polarization with horizontal (a) and vertical (b) pump beam orientation. In the first case, the ellipticity parameter of the polarization was 0.1 and in the second case, it was 0.23.

Figures 1(a) and 1(b) show that the main axis of the THz ellipse was in the same position as the fundamental pump polarization axis [19]. The ellipticity of the THz radiation increased with an increase in the fundamental pump polarization ellipticity. Varying the pump beam ellipticity, the ellipticity of the THz pulses could be controlled and changed. Additionally, doubling the fundamental harmonic ellipticity led to a doubling of the THz harmonic ellipticity. The THz radiation beam at the filament generation had high spatial homogeneity in the center of the filament [31]. Besides, the THz field propagation from the filament had a conical structure [29] that created a “donut” vortex beam shape after collimation. Using the THz pulse time-domain holography method [3] one could obtain the THz field distribution in each spatial coordinate, which provided the polarization distribution pictures. The measurement area of the THz signal at every point was 5 mm in diameter (Fig. 3(a)). Fig. 3(b,c) shows

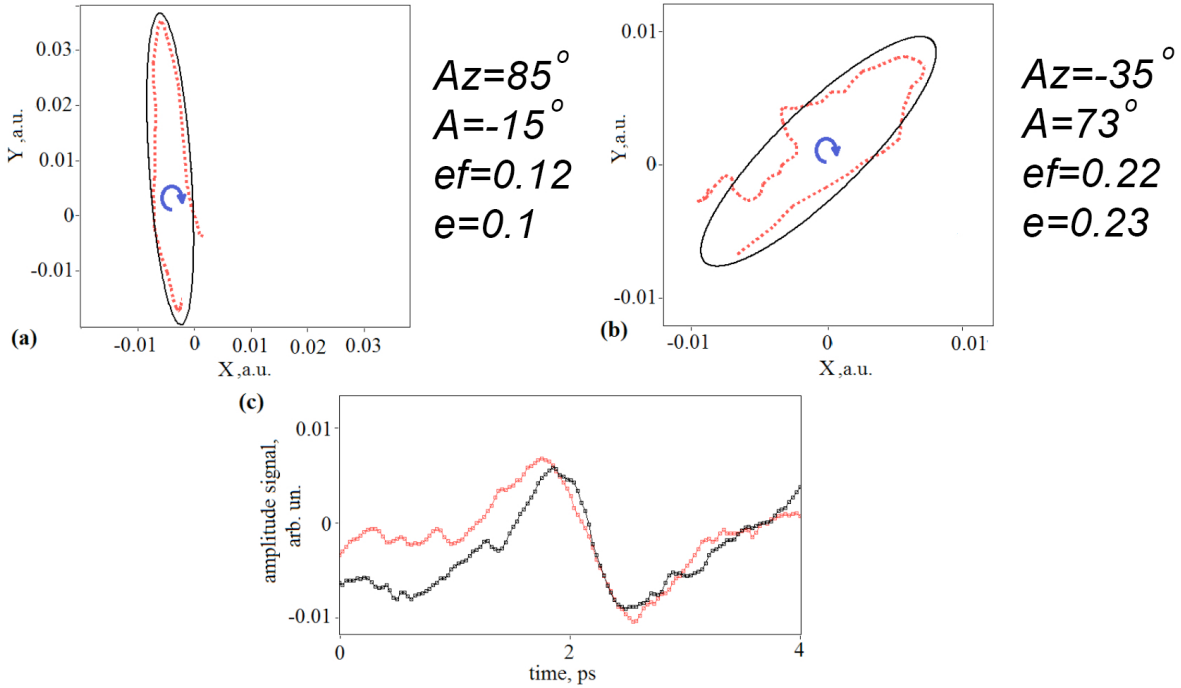


FIG. 1. (Color online) Measurement results (red dots) and approximation (black line) of the THz polarization for the case of horizontal pump polarization (a); Measurement results (red dots) and approximation (black line) of the THz polarization for the case of the vertical pump polarization (b); The THz field for two orthogonal THz polarizer states for the vertical pump polarization (red dots at  $0^\circ$ , black dots at  $90^\circ$ ) (c).  $e$  is the ellipticity parameter of the THz beam profile polarization, Azimuth is the polarization angle of the THz beam profile radiation.  $ef$  is the ellipticity parameter of polarization of the fundamental harmonic,  $\alpha$  is the angle of fundamental harmonic polarization

that spectra in different donut-beam profile positions are the same and temporal profiles differ only in phase shift which can be explained by the vortex structure of the generating beam in two-color filamentation. In the spectral domain, the polarization state of the generated THz beam exhibited no frequency dependency, for example, for point number 7 (Fig. 3(a)) the polarization had a constant value equal to  $\sim 0.09$  in our frequency range of 0.15–2.00 THz. Therefore, it is possible to determine the polarization characteristics of the THz beam considering only a temporal form of the wave-packet. Fig. 4 illustrates the spatial distribution of the THz beam polarization for two polarization states of the pump beam radiation.

These results show that even though the THz polarization retained aperture integral ellipticity in the spatial distribution, there was still an inhomogeneity in the polarization states. However, the tilt angle for each spatial point of the THz field has the same value. Moreover, the polarization ellipse of the spatial distribution of the THz field changes from the quasi-linear state to the high-elliptical state and back during radial bypass with a period equal to  $2\pi$ . Such spatial inhomogeneity is determined by the initial inhomogeneous spatial distribution of the polarization in the pump-fundamental harmonic. This was confirmed by the direct dependence of the polarization of the THz field on the polarization of the fundamental harmonic [14]. The observed inhomogeneity in the fundamental harmonic was determined by the fact that after the focusing lens, the fundamental harmonic beam became spherical and there was a polarization spatial dependence owing to the  $\beta$ -BBO crystal acting as a phase plate (Fig. 4).

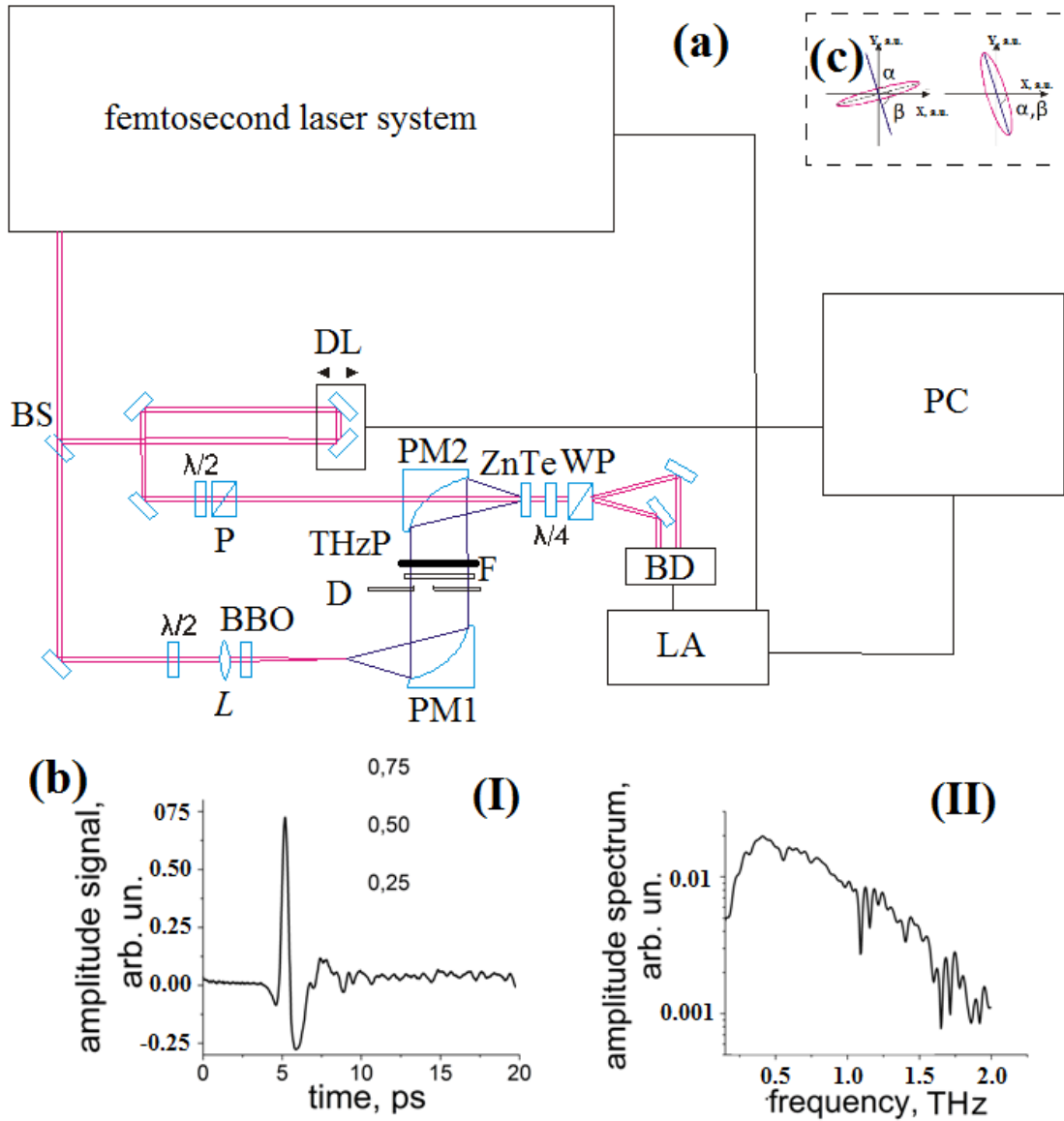


FIG. 2. (Color online) The experimental setup for measuring the spatial distribution of polarization of the THz radiation generated in two-color filamentation (a). BS is the beam splitter, DL is the time delay line, P is Glan prism,  $\beta$ -BBO is a nonlinear crystal for the second harmonic generation (Barium borate), L is a lens, PM1 and PM2 are parabolic mirrors, D is a diaphragm, THzP is a terahertz polarizer (wire grid), F is a Teflon filter, WP is a Wollaston prism, BD is a balance detector, LA is a Lock-in amplifier, PC is a computer. The temporal (I) and spectral (II) forms of the initial integrated beam profile THz pulse (b). Polarization of the fundamental and second harmonics (c): case of the initial horizontal (c-inset left) and vertical (c-inset right) polarization of the fundamental harmonic;  $\alpha$  is the angle of the main axis inclination of the polarization ellipse of the fundamental harmonic after the  $\beta$ -BBO crystal ( $\alpha = -15^\circ$  for horizontal polarization;  $\alpha = 73^\circ$  for vertical polarization),  $\beta$  is the angle of inclination of the linear polarization of the second harmonic after the  $\beta$ -BBO crystal ( $\beta = 73^\circ$ )

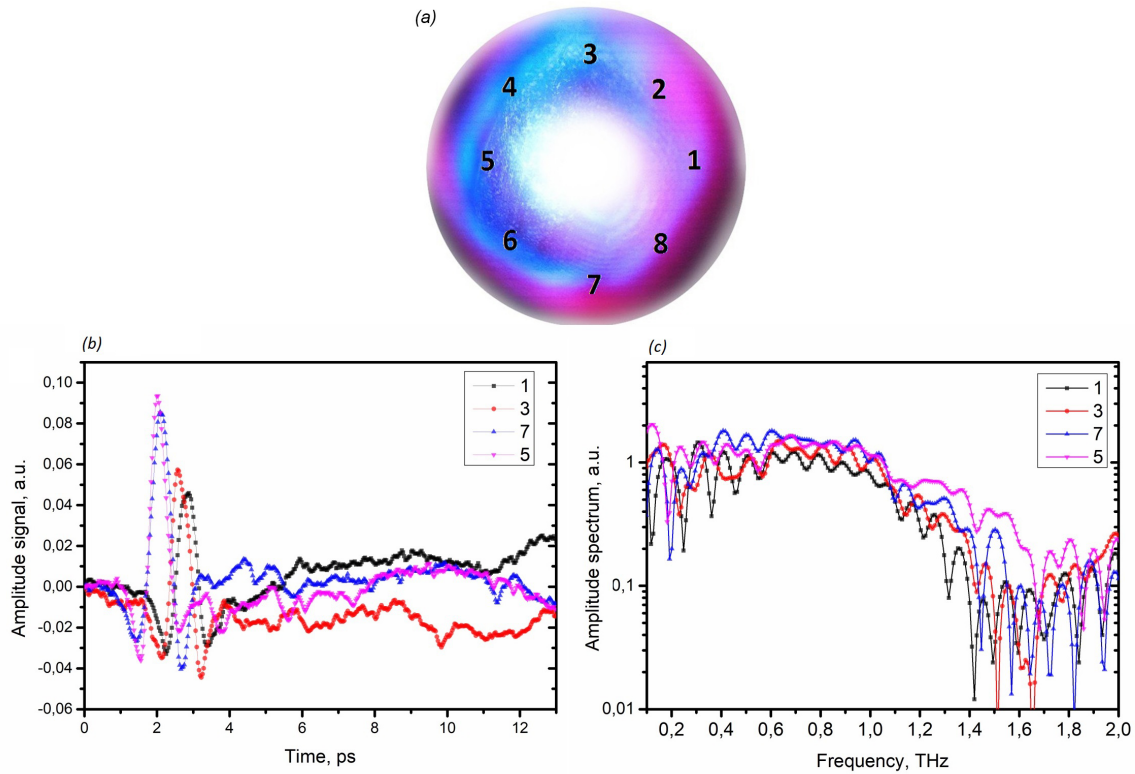


FIG. 3. (Color online) Measurement areas of a two-color filament and the areas of polarization measurement; Spatial polarization distribution of the THz beam for the two polarization states of the pump beam radiation corresponding to the points (1–8) from (a). Temporal (b) and spectral (c) form in different beam profile positions of the donut structure corresponding to (a)

### 3. Conclusion

Spatial distribution of the polarization of the terahertz radiation from a two-color filament in air generated by a femtosecond laser is experimentally measured in our study. We show that for this setup, the spatial inhomogeneity of the THz field is affected by the spatial inhomogeneity of the fundamental harmonic polarization. The inhomogeneity of the fundamental harmonic polarization is formed because of the passage of the spherical front after the focusing lens through the  $\beta$ -BBO crystal. In this case, the crystal acts as a phase plate for the beam profile. The management of the fundamental harmonic polarization can assist control of the polarization of the THz field and to form vortex beams. For instance, the conversion method of THz vortex beam generation was demonstrated in [22], where the sign of the topological charge could be controlled. This is made possible by conversion of the radially polarized THz beam via optical element achromatic polarization.

### Acknowledgements

We thank X.-C. Zhang for consultation with the experiment. This work was partially financially supported by the Government of the Russian Federation, Grant 074-U01 and Project 3.9041.2017/7.8.

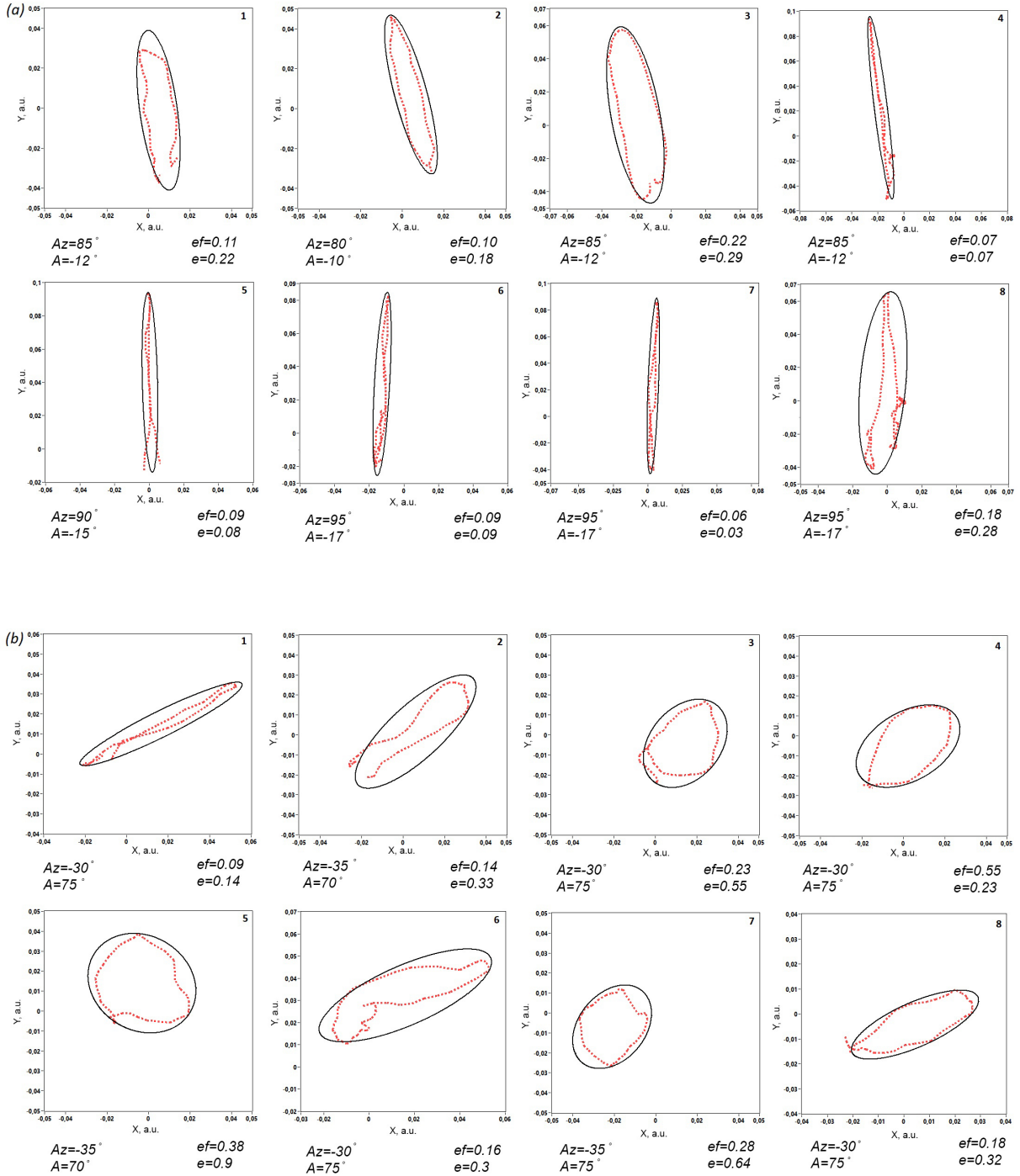


FIG. 4. (Color online) Spatial polarization distribution of the THz beam for the two polarization states of the pump beam radiation corresponding to the points (1–8) from (Fig. 3(a)). (a) – corresponds to the angle of the main axis inclination of the polarization ellipse of the fundamental harmonic after the  $\beta$ -BBO crystal  $\alpha = -15^\circ$  with the ellipticity of 0.12 (see Fig. 2(b-I)). (b) – corresponds to the angle  $\alpha = 73^\circ$  with the ellipticity of 0.22 (see Fig. 2(b-II)).  $e$  is ellipticity parameter of the polarization of the THz radiation,  $Az$  is the angle of polarization of the THz radiation,  $ef$  is the ellipticity parameter of polarization of the fundamental harmonic,  $A$  is the angle of polarization of the fundamental harmonic

## References

- [1] Siegel P.H. Terahertz technology in biology and medicine. *IEEE Transactions on Microwave Theory and Techniques*, 2004, **52** (10), P. 2438–2447.
- [2] Gredukhina I.V., Plotnikova L.V., et al. Influence of the degree of neutralization of acrylic acid and cross-linking agent on optical properties and swelling of sodium polyacrylate. *Optics and Spectroscopy*, 2017, **122** (6), P. 877–879.
- [3] Petrov N.V., Kulya M.S., et al. *IEEE Transactions on Terahertz Science and Technology*, 2016, **6** (3), P.464–472.
- [4] Balbekin N.S., Kulya M.S., Rogov P.Y., Petrov N.V. The modeling peculiarities of diffractive propagation of the broadband terahertz two-dimensional field. *Physics Procedia*, 2015, **73**, P. 49–53.
- [5] Kulya M.S., Balbekin N.S., et al. Computational terahertz imaging with dispersive objects. *Journal of Modern Optics*, 2017, **64**, P. 1283–1288.
- [6] Kulya M.S., Petrov N.V., Tcypkin A.N., Bepalov V.G. Influence of raster scan parameters on the image quality for the THz phase imaging in collimated beam with a wide aperture. *Journal of Physics: Conference Series*, 2014, **536** (1), P. 012010.
- [7] Semenova V.A., Kulya M.S., Bepalov V.G. Numerical simulation of broadband vortex terahertz beams propagation. *Journal of Physics: Conference Series*, 2016, **735** (1), P. 012064.
- [8] Cook D.J., Hochstrasser R.M. Intense terahertz pulses by four-wave rectification in air. *Optics Letters*, 2000, **25** (16), P. 1210–1212.
- [9] Lu X., Zhang X.C. Investigation of ultra-broadband terahertz time-domain spectroscopy with terahertz wave gas photonics. *Frontiers of Optoelectronics*, 2014, **7** (2), P. 121–155.
- [10] Roskos H.G., Thomson M.D., Kreß M., Löffler A.T. Broadband THz emission from gas plasmas induced by femtosecond optical pulses: From fundamentals to applications. *Laser & Photonics Reviews*, 2007, **1** (4), P. 349–368.
- [11] Thomson M.D., Blank V., Roskos H.G. Terahertz white-light pulses from an air plasma photo-induced by incommensurate two-color optical fields. *Optics Express*, 2010, **18** (22), P. 23173–23182.
- [12] Liu W., Théberge F., et al. An efficient control of ultrashort laser filament location in air for the purpose of remote sensing. *Applied Physics B: Lasers and Optics*, 2006, **85** (1), P. 55–58.
- [13] Couairon A., Mysyrowicz A. Femtosecond filamentation in transparent media. *Physics Reports*, 2007, **441** (2), P. 47–189.
- [14] D'Amico C., Houard A., et al. Conical forward THz emission from femtosecond-laser-beam filamentation in air. *Physical Review Letters*, 2007, **98** (23), P. 235002.
- [15] Andreev A.A., Bepalov V.G., et al. Generation of ultrabroadband terahertz radiation under optical breakdown of air by two femtosecond pulses of different frequencies. *Optics and Spectroscopy*, 2009, **107** (4), P. 538–544.
- [16] Amico C.D., Houard A., et al. Forward THz radiation emission by femtosecond filamentation in gases: theory and experiment. *New Journal of Physics*, 2008, **10** (1), P. 013015.
- [17] Zhang Y., Chen Y., et al. Non-radially polarized THz pulse emitted from femtosecond laser filament in air. *Optics Express*, 2008, **16** (20), P. 15483–15488.
- [18] Chen Y., Marceau C., et al. Elliptically polarized terahertz emission in the forward direction of a femtosecond laser filament in air. *Applied Physics Letters*, 2008, **93** (23), P. 231116.
- [19] Béjot P., Kasparian J., Wolf J.P. Dual-color co-filamentation in Argon. *Optics express*, 2008, **16** (18), P. 14115–14127.
- [20] Dietze D., Darmo J., et al. Polarization of terahertz radiation from laser generated plasma filaments. *JOSA B*, 2009, **26** (11), P. 2016–2027.
- [21] Stremoukhov S., Andreev A., et al. Origin of ellipticity of high-order harmonics generated by a two-color laser field in the cross-polarized configuration. *Physical Review A*, 2016, **94** (1), P. 013855.
- [22] Imai R., Kanda N., et al. Generation of broadband terahertz vortex beams. *Optics Letters*, 2014, **39** (13), P. 3714–3717.
- [23] Semenova V.A., Kulya M.S., Bepalov V.G. Numerical simulation of broadband vortex terahertz beams propagation. *Journal of Physics: Conference Series*, 2016, **735** (1), P. 012064
- [24] Semenova V.A., Kulya M.S., et al. Amplitude-phase imaging of pulsed broadband terahertz vortex beams generated by spiral phase plate. *41st International Conference on Infrared, Millimeter and Terahertz Waves (IRMMW-THz)*, 2016, 7758823.
- [25] He J., Wang X., et al. Generation and evolution of the terahertz vortex beam. *Optics Express*, 2013, **21** (17), P. 20230–20239.
- [26] Oh T.I., You Y.S., Kim K.Y. Two-dimensional plasma current and optimized terahertz generation in two-color photoionization. *Optics Express*, 2012, **20** (18), P. 19778–19786.
- [27] Wu Q., Hewitt T.D., Zhang X.C. Two-dimensional electro-optic imaging of THz beams. *Applied Physics Letters*, 1996, **69** (8), P. 1026–1028.
- [28] Gorodetsky A., Koulouklidis A.D., Massaoui M., Tzortzakis S. Physics of the conical broadband terahertz emission from two-color laser-induced plasma filaments. *Physical Review A*, 2014, **89** (3), P. 033838.
- [29] Zhang Y., Sun W., Zhang Y. Spectra modulation of terahertz radiation from air plasma. In *SPIE/COS Photonics Asia*, 2016, P. 1003025–1003025.
- [30] Chen Y., Marceau C., et al. Polarization separator created by a filament in air. *Optics Letters*, 2008, **33** (23), P. 2731–2733.
- [31] Théberge F., Aközbe N., et al. Tunable ultrashort laser pulses generated through filamentation in gases. *Physical Review Letters*, 2006, **97** (2), P. 023904.